

Kinetics, Mechanism, and Thermodynamics of the Reversible Reaction of Methylglyoxal (CH₃COCHO) with S(IV)

Eric A. Betterton and Michael R. Hoffmann*

Environmental Engineering Science, W. M. Keck Laboratories, California Institute of Technology, Pasadena, California 91125 (Received: October 27, 1986; In Final Form: January 19, 1987)

At pH ≤ 2 the following rate law for the formation of hydroxyacetylmethanesulfonate (HAMS) from methylglyoxal (MG) and S(IV) (H₂O-SO₂, HSO₃⁻, SO₃²⁻) is obtained: $d[\text{HAMS}]/dt = (((k_0\alpha_1[\text{H}^+]/K_{a0}) + k_1\alpha_1 + k_2\alpha_2)[\text{S(IV)}][\text{MG}]_0)/((1 + K_d + K_d[\text{H}^+]/K_{a0}))$, where α_1 and α_2 are the fractional concentrations of HSO₃⁻ and SO₃²⁻, respectively; k_0 is the rate constant for the reaction of HSO₃⁻ with the carbocation aldehyde species (CH₃COC⁺HOH); k_1 and k_2 are the rate constants for the reaction of unhydrated MG with HSO₃⁻ and SO₃²⁻, respectively; K_d is the dehydration constant of hydrated MG; and K_{a0} is the acid dissociation constant of the carbocation. At pH ≥ 4 the rate of formation of HAMS is determined by the rate of dehydration of the diol form of (hydrated) MG: $d[\text{HAMS}]/dt = k_d[\text{MG}]/(1 + K_d + K_d[\text{H}^+]/K_{a0})$, where $k_d = k_w + k_H[\text{H}^+] + k_{OH}[\text{OH}^-] + k_A[\text{A}] + k_B[\text{B}]$, and k_w is the intrinsic (water) rate constant; k_H and k_{OH} are the specific acid and base rate constants; and k_A and k_B are the general acid (A) and base (B) rate constants. Between pH 2 and 4, biexponential kinetics are observed because, under our conditions, the rates of dehydration and of S(IV) addition become comparable. Over the pH range 0.7-7.0, the dissociation of HAMS follows the rate law: $d[\text{S(IV)}]/dt = ((k_{-0}[\text{H}^+] + k_{-1} + k_{-2}K_{a3}/[\text{H}^+])K_{a4}[\text{H}^+][\text{HAMS}])/([\text{H}^+]^2 + K_{a4}[\text{H}^+] + K_{a3}K_{a4})$, where k_{-0} , k_{-1} , and k_{-2} are the reverse of the analogous forward rate constants defined above and K_{a3} and K_{a4} are the acid dissociation constants of the sulfonate anion and the sulfonic acid, respectively. Experiments to determine the effect of temperature on the rate (and equilibrium) constants indicate a marked effect of ΔS^\ddagger (and ΔS_{298}) on the relative magnitude of these constants.

Introduction

The bisulfite adduct of formaldehyde, hydroxymethanesulfonate, has recently been identified in fog and rain water collected in polluted environments and it has been suggested that the adduct may be an important reservoir for S(IV), i.e., SO₂·H₂O, HSO₃⁻, and SO₃²⁻, in aqueous droplets in the atmosphere.¹ This prompted a detailed investigation of the kinetics of the formation of hydroxymethanesulfonate² and also of the analogous adduct derived from benzaldehyde, α -hydroxyphenylmethanesulfonate.³ It has become apparent during the course of these studies that for an aldehyde to be important as a S(IV) reservoir it should satisfy three conditions. First, it should occur in the environment at a significant concentration, second it should have a relatively high effective Henry's law constant (the combination of the intrinsic Henry's law constant and the hydration constant), and third it should react rapidly with S(IV) to form a stable adduct. Formaldehyde satisfies these three conditions but benzaldehyde, which appears to have a low effective Henry's law constant and a relatively low affinity for S(IV), does not.

Laboratory studies⁴ have shown that, in the gas phase, OH[•] reacts with substituted aromatic hydrocarbons such as toluene (which are ubiquitous in the environment)⁵ to generate ring-cleavage products which include the α -dicarbonyl aldehydes, methylglyoxal (CH₃COCHO) and glyoxal (CHOCHO). Methylglyoxal may also be a product of the photooxidation of isoprene, an important naturally occurring hydrocarbon.⁶ Although the α -dicarbonyls are themselves subject to photochemical decomposition,⁷ they have recently been found in rain, fog, and mist droplets.⁸

Methylglyoxal and glyoxal have very large hydration constants⁹ and so the effective Henry's law constant for these aldehydes is also likely to be large; but little is known about the glyoxal-S(IV) reaction and the methylglyoxal-S(IV) reaction has not been studied at all. Glyoxal and formaldehyde are reported¹⁰ to react with S(IV) at about the same rate, and the two successive apparent stability constants for glyoxal-S(IV) adduct formation are $K_1 > 3.7 \times 10^3 \text{ M}^{-1}$ and $K_2 = 3.7 \times 10^3 \text{ M}^{-1}$ at pH 7.3, 20 °C, and unspecified ionic strength μ . We expected that the (single) apparent stability constant for methylglyoxal-S(IV) adduct formation would also be $> 3.7 \times 10^3 \text{ M}^{-1}$ and so both α -dicarbonyl aldehydes showed the potential for being important S(IV) reservoirs.

The primary aim of this work is to investigate the thermodynamics and kinetics of the aqueous methylglyoxal-S(IV) reaction under conditions most applicable to natural systems (i.e., acidic to neutral pH). (The glyoxal-S(IV) reaction will be the subject of a separate report.) Previous studies of aldehyde-S(IV) chemistry have been devoted almost exclusively to formaldehyde^{2,11} or to benzaldehyde^{3,12} (and its derivatives),^{3,13} the only other aliphatic aldehyde that appears to have been studied in any detail is isobutyraldehyde.¹⁴ Thus, a secondary aim of this work is to extend the range of aldehydes for this important reaction which is commonly used to separate and purify aldehydes and reactive ketones. The final aim of this study is to assess the potential importance of methylglyoxal as a S(IV) reservoir and to point out other potentially important aldehydes.

The methylglyoxal-S(IV) system is conveniently discussed in terms of three types of reaction, viz., dehydration of the diol (CH₃COCH(OH)₂), formation of the adduct by reaction of S(IV)

(1) Munger, J. W.; Tiller, C.; Hoffmann, M. R. *Science* **1986**, *231*, 247-9.

(2) Boyce, S. D.; Hoffmann, M. R. *J. Phys. Chem.* **1984**, *88*, 4740-6.

(3) Olson, T. M.; Boyce, S. D.; Hoffmann, M. R. *J. Phys. Chem.* **1986**, *90*, 2482-8.

(4) (a) Tuazon, E. C.; Atkinson, R.; MacLeod, H.; Biermann, H. *Environ. Sci. Technol.* **1984**, *18*, 981-4. (b) Tuazon, E. C.; MacLeod, H.; Atkinson, R.; Carter, W. P. L. *Environ. Sci. Technol.* **1986**, *20*, 383-7. (c) Gery, M. W.; Fox, D. L.; Jeffries, H. E.; Stockburger, L.; Weathers, W. S. *Int. J. Chem. Kinet.* **1985**, *17*, 931-55.

(5) (a) Lonneman, W. A.; Bellar, T. A.; Altschuller, A. P. *Environ. Sci. Technol.* **1968**, *2*, 1017-20. (b) Lonneman, W. A.; Koczyński, S. L.; Darley, P. E.; Sutterfield, F. D. *Environ. Sci. Technol.* **1974**, *8*, 229-236.

(6) Lloyd, A. C.; Atkinson, R.; Lurmann, F. W.; Nitta, B. *Atmos. Environ.* **1983**, *17*, 1931-50.

(7) Plum, C. N.; Sanhueza, E.; Atkinson, R.; Carter, W. P. L.; Pitts, J. N. *Environ. Sci. Technol.* **1983**, *17*, 479-84.

(8) Steinberg, S.; Kaplan, I. R. *Int. J. Environ. Anal. Chem.* **1984**, *18*, 253-66.

(9) Wasa, T.; Musha, S. *Bull. Univ. Osaka Prefect. Ser. A* **1970**, *19*, 169-80.

(10) Salomaa, P. *Acta Chem. Scand.* **1956**, *10*, 306-10.

(11) (a) Sørensen, P. E.; Andersen, V. S. *Acta Chem. Scand.* **1970**, *24*, 1301-6. (b) Wagner, C. *Ber. Dtsch. Chem. Ges.* **1929**, *62*, 2873-7. (c) Jones, P.; Oldham, K. B. *J. Chem. Educ.* **1963**, *40*, 366-7. (d) Skrabal, A.; Skrabal, R. *Sitz. Akad. Wers. Wien.* **1936**, *145*, 617-47. (e) Deister, U.; Neeb, R.; Helas, G.; Warneck, P. *J. Phys. Chem.* **1986**, *90*, 3213-7. (f) Kok, G. L.; Gitlin, S. N.; Lazrus, A. L. *J. Geophys. Res.* **1986**, *91*, 2801-4. (g) Dong, S.; Dasgupta, P. K. *Atmos. Environ.* **1986**, *20*, 1635-7.

(12) (a) Stewart, T. D.; Donnally, L. H. *J. Am. Chem. Soc.* **1932**, *54*, 2333-40. (b) *J. Am. Chem. Soc.* **1932**, *54*, 3555-8. (c) *J. Am. Chem. Soc.* **1932**, *54*, 3559-68. (d) Sousa, J. A.; Margerum, J. D. *J. Am. Chem. Soc.* **1959**, *81*, 3013-6.

(13) Young, P. R.; Jencks, W. P. *J. Am. Chem. Soc.* **1977**, *99*, 1206-14.

(14) Green, L. R.; Hine, J. *J. Org. Chem.* **1974**, *39*, 3896-901.

with the unhydrated aldehyde, and dissociation of the adduct. Each of these areas was studied separately and the ratio of the formation rate constant to the dissociation rate constant was used to calculate the stability constant. This is in contrast to previous studies which used a measured stability constant and a measured rate constant (either forward or reverse) to calculate the other rate constant.

Experimental Procedure

Materials. A.R. grade reagents were used except where indicated and high-purity (18 M Ω cm) deionized water was obtained from a Millipore MilliRO-4 MilliQ system. Buffers were prepared¹⁵ from HCl/NaCl (pH 0.7–2.0), ClCH₂COOH/NaOH (pH 2.5–3.5), CH₃COOH/NaOH (pH 4.0–5.5), and NaH₂PO₄·H₂O/Na₂HPO₄·7H₂O (pH 5.6–7.0). They were deoxygenated with a stream of nitrogen and filtered (0.2 μ m Nucleopore) before use. In the case of chloride, acetate, and phosphate the buffer contributed the entire ionic strength of 0.2 M, but for chloroacetate the total buffer concentration (ClCH₂COOH + ClCH₂COONa) was 0.05 M. The ionic strength was adjusted to 0.2 M with NaCl which was also used to maintain the ionic strength at 0.2 M for the acetate, sulfite, and phosphate catalysis experiments.

S(IV) solutions were freshly prepared from NaHSO₃ or Na₂SO₃ and used immediately. They were occasionally analyzed by titration with As₂O₃-standardized I₂ solution;¹⁶ it was found that even for NaHSO₃ the theoretical and actual S(IV) concentrations agreed. The rate of oxidation of S(IV) to S(VI) was minimized by storing the solutions under nitrogen and by adding 10⁻⁵ M EDTA (to retard trace-metal-catalyzed oxidation).¹⁷ EDTA had no observable effect on the kinetics.

Methylglyoxal (MG) (Sigma; 40% aqueous solution) was stored in the dark at 5 °C and was used without further purification. An aqueous stock solution (1.36 M) was standardized by titration with excess NaHSO₃ followed by rapid back-titration at low pH with I₂. The method is the same as that described by Salomaa¹⁰ for the determination of glyoxal except that no correction for the presence of unreacted aldehyde was necessary. The stock solution was stored in the dark at room temperature. No evidence of deterioration was found over a period of several months.

Sodium hydroxyacetylmethanesulfonate (HAMS) was prepared by a method similar to that of Steinbauer and Prey.¹⁸ A solution of 8.13 g of NaHSO₃ (0.08 mol) in 25 mL of H₂O was slowly added to 13.8 mL of 40% aqueous methylglyoxal (0.09 mol) and allowed to stand at room temperature in a sealed flask for 24 h. The solution was evaporated (20 mbar, 40 °C) to a syrup, 50 mL anhydrous ethanol was added, and the evaporation was repeated. The resulting viscous liquid was stirred with 50 mL of ethanol to precipitate a white solid which was filtered on sintered glass and washed successively with ethanol and anhydrous diethyl ether. The hygroscopic powder was stored over silica gel in a desiccator. Yields were 80–90%. The results of elemental analysis (Galbraith Laboratories Inc., Knoxville, TN) of two separate batches were the same and, based on % C, indicate the presence of a single molecule of water of crystallization: (% found, % calculated for CH₃COCH(OH)SO₃Na·H₂O): C (18.47, 18.56); H (2.97, 3.63); S (19.05, 16.52); Na (13.93, 12.42). Titration of the salt with excess I₂ and back-titration with Na₂S₂O₃¹⁶ showed that the [S(IV)] was consistent with this formula, i.e., only the monobisulfite adduct was formed, but the method was not sensitive enough to precisely determine the number of molecules of water of crystallization which will be taken to be unity.

Methods. A Radiometer PHM84 pH meter and a Radiometer GK2421C combined pH electrode were calibrated with Radiometer pH 4.01 and pH 7.00 buffers. Unless otherwise stated, the temperature of all solutions was 25.0 \pm 0.1 °C maintained with Haake water baths. Kinetic results are normally the average of at least three experiments.

The rate of dehydration of the diol form of methylglyoxal (CH₃COCH(OH)₂) was determined by measuring the rate of increase of A₂₈₅, the absorbance at 285 nm, (λ_{\max} for HAMS; $\epsilon_{285} \sim 57$ M⁻¹ cm⁻¹) which occurred when aqueous methylglyoxal reacted with excess S(IV) (see Results section for concentration ranges). The method is based on that of Bell and Evans¹⁹ who used S(IV) as a scavenger to study the analogous dehydration of methylene glycol. Plots of ln(A_∞ - A) vs. time were linear (*r*² \geq 0.99) over 3–4 half-lives from pH 4 to pH 7 and the slope of these plots gave *k*_{obsd}.

Below about pH 3.5 the kinetic traces became biexponential and the two observed macroscopic rate constants *k*_{obsd1} (due to the first reaction) and *k*_{obsd2} (due to the second reaction) were separated by the normal methods.²⁰ Plots of ln(A - A_∞) vs. time (at long time periods) gave *k*_{obsd2} and plots of ln(A' - A_∞) gave *k*_{obsd1} where A' is the absorbance corrected for the second reaction. In both cases straight lines were obtained over 3–4 half-lives. At the relatively low pH of these experiments the intense absorption of SO₂·H₂O ($\epsilon_{276} = 3.88 \times 10^2$ M⁻¹ cm⁻¹)²¹ dominated the spectrum and A₂₈₅ decreased with time as S(IV) was consumed. It became increasingly difficult to accurately record the small relative absorbance change as the pH was lowered further and these experiments were not pursued.

The rate of formation of HAMS (at pH < 2.5) was monitored at 285 nm by UV-visible spectrophotometry with [S(IV)] \ll [methylglyoxal] (the concentration ranges are given in the Results section). The reaction was initiated by injecting the appropriate volume (a few microliters) of NaHSO₃ into 3.00 mL of aqueous buffered methylglyoxal which was thermostated in a sealed quartz cuvette. Oxygen was excluded by using syringe-septa techniques. A blank run in the absence of methylglyoxal showed no change in absorbance with time.

The rate of dissociation of HAMS was studied by measuring the rate of formation of I⁻ or the rate of loss of I₂ when HAMS dissociated in I₂ solution:



Reaction 1b is extremely fast (*k* = 2.3 $\times 10^9$ M⁻¹ s⁻¹)²² compared to reaction 1a, which is consequently the rate-determining step in the formation of I⁻ or the loss of I₂. There is no kinetic distinction between I₂ and I₃⁻ in this respect since I₃⁻ also reacts with HSO₃⁻ very rapidly (*k* = 2.2 $\times 10^7$ M⁻¹ s⁻¹).²²

Between pH 0.7 and pH 5.5 the rate of dissociation of HAMS was slow enough to be measured with an ion-selective electrode. An Orion 94-53 iodide electrode and Orion 90-02-00 double-junction reference electrode were fitted into a sealed 50-mL water-jacketed glass cell which was magnetically stirred. The test solution almost filled the cell so that little head space remained and I₂ loss through vaporization, and oxidation of I⁻ by O₂ were minimized. A kinetic run was initiated by injecting a small volume of HAMS solution (at pH \sim 2 to minimize the rate of dissociation) through a Teflon-lined rubber septum into 50.00 mL of I₂ solution buffered at the appropriate pH and recording the rate of change of the electrode potential using an Orion Ionalyzer/901 meter.

(15) (a) Long, C., Ed. *Biochemists' Handbook*; E. & F. Spon: London, 1961. (b) Perrin, D. D.; Dempsey, B. *Buffers for pH and Metal Ion Control*; Chapman and Hall: London, 1974.

(16) (a) Vogel, A. I. *Quantitative Inorganic Analysis*, 3rd ed.; Wiley: New York, 1961. (b) Greenberg, A. E., Trussell, R. R., Clesceri, L. S., Ed. *Standard Methods for the Examination of Water and Wastewater*, 16th ed.; American Public Health Association: Washington, 1985.

(17) Hoffmann, M. R.; Boyce, S. D. In *Trace Atmospheric Constituents: Properties Transformations and Fates*; Schwartz, S. E., Ed.; Wiley: New York, 1983; pp 147–89.

(18) Steinbauer, E.; Prey, V. *Monatsch. Chem.* **1962**, *93*, 303–11.

(19) Bell, R. P.; Evans, P. G. *Proc. R. Soc. London Ser. A* **1966**, *291*, 297–323.

(20) (a) Hiromi, K. *Kinetics of Fast Enzyme Reactions*; Halsted: Tokyo, 1979. (b) Moore, J. W.; Pearson, R. G. *Kinetics and Mechanism*, 3rd ed.; Wiley-Interscience: New York, 1981. (c) *Ibid.*, p 290. The derivation assumes that [CH₃COCHO]₀ = 0 which is not strictly true in this case but which is a good approximation.

(21) Seo, E. T.; Sawyer, D. T. *J. Electroanal. Chem.* **1964**, *7*, 184–9.

(22) Bunau, G. v.; Eigen, M. *Z. Phys. Chem. (Frankfurt/Main)* **1962**, *32*, 25–50.

The HAMS solution was used within 2 min of being prepared.

At pH < 3 the half-life of the reaction was too long (≥ 1.5 h) to allow stable and repeatable end-point readings to be obtained (the problem seemed to be associated with electrode drift) and the experimental technique was modified. A stock of the HAMS/I₂ solution was quickly transferred into a series of flasks which were filled (without head space) sealed and protected from the light. The flasks were thermostated in a water bath and at intervals their contents were analyzed for I⁻ (with the electrode) and discarded. At the end of each run a calibration curve of the measured potential (mV) vs. log [I⁻] was constructed for each pH (and temperature) with freshly prepared standard KI solutions. The plots were linear over the several decade units applicable to these experiments and gave mV_I (intercept) and *S* (slope).

The iodide concentration at time *t*, [I⁻]_{*t*}, is related to the observed electrode voltage (mV_{*t*}) by eq 2a which is based on the

$$\ln [I^-]_t = \frac{(mV_t - mV_I)2.303}{S} \quad (2a)$$

$$\ln ([S(IV)]_\infty - [S(IV)]_t) = k_{\text{obsd}}t + \ln [S(IV)]_\infty \quad (2b)$$

$$\ln [\exp(2.303(mV_\infty - mV_t)/S) - \exp(2.303(mV_t - mV_I)/S)] = -kt + C \quad (2c)$$

Nernst equation. This is readily substituted into the first-order rate eq 2b to give eq 2c where mV_∞ is the end-point potential measured after > 6 half-lives, and *C* is a constant. Plots of the left side of eq 2c vs. *t* were linear over 3–4 half-lives. The calculated [I⁻]_∞ (from the known [HAMS]) and the observed [I⁻]_∞ were in good agreement.

At higher pH (≥ 5.6) the rate of dissociation of HAMS was too high to follow conveniently with the ion-selective electrode, and stopped-flow spectrophotometry was used to measure the rate of disappearance of the I₂/I₃⁻ peak at 449 nm.²³ One syringe contained I₂ in the appropriate buffer while the other contained HAMS in 0.01 M HCl ($\mu = 0.2$ M; NaCl). All solutions were freshly prepared and were protected from the light. The pH of the mixed solutions (the effluent from the stopped-flow apparatus) was measured. Duplicate experiments at pH 3.0 showed no difference between results obtained by the ion-selective electrode method and those obtained by UV-visible spectrophotometry and the (nearly overlapping) results obtained at pH 5.5 and 5.6 by ion-selective electrode and by stopped-flow, respectively, showed no systematic error.

The equilibrium constants (*K*) used in the calculations in this work have been corrected from $\mu = 0$ (*K*⁰) to $\mu = 0.2$ M using the Davies equation²⁴ to calculate the activity coefficients γ :

$$\log \gamma = -Az^2[(\mu^{1/2}/(1 + \mu^{1/2})) - 0.2\mu] \quad (3)$$

A = 0.509 for water at 25 °C and *z* = ionic charge. [H⁺] (in the experimentally observed kinetic data) refers to the measured hydrogen ion activity (-log pH) and was not corrected, e.g., $K_{\text{HSO}_3^-} = K^0_{\text{HSO}_3^-}/\gamma_{\text{HSO}_3^-}$ and $K_{\text{SO}_3^{2-}} = K^0_{\text{SO}_3^{2-}}/\gamma_{\text{SO}_3^{2-}}$. Equilibrium and thermodynamic data are summarized in Table I.

Results

At low pH (≤ 2.0) the rate of formation of HAMS from MG and S(IV) is determined by the rate of the S(IV) addition reaction while at high pH (≥ 4.0) the rate of formation of HAMS is determined by the rate of dehydration of the diol form of MG (evidence for this will be given later). At intermediate pH

TABLE I: Equilibrium Constants and Thermodynamic Data

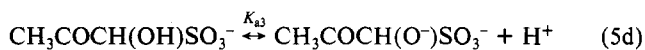
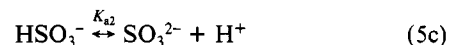
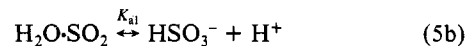
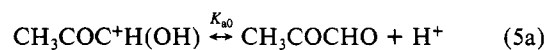
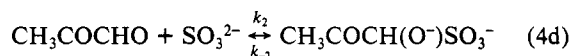
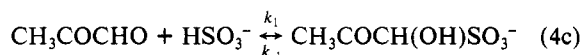
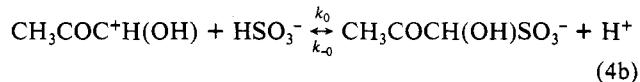
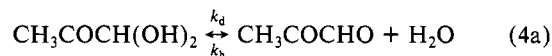
acid A ^a	<i>K</i> _a ^{0, b} M	<i>K</i> _a ^c M	ΔH_{298} , kJ/mol	ref
H ₂ O·SO ₂	1.23×10^{-2}	1.68×10^{-2}	-16.7	25a
HSO ₃ ⁻	6.61×10^{-8}	1.69×10^{-7}	-12.6	25a
CH ₃ COOH	1.75×10^{-5}	2.40×10^{-5}		25b
H ₂ PO ₄ ⁻	6.32×10^{-8}	1.61×10^{-7}		25a
CH ₃ COCH(OH)SO ₃ ⁻		1.93×10^{-11}	-20 ^d	26

equilibrium	<i>K</i> ^e	ΔH_{298} , kJ/mol	ref
SO ₂ (g) ↔ SO ₂ (aq)	1.1	-25.1	25a
HCHO(g) ↔ HCHO(aq)	2.5		27
HCHO(aq) ↔ HCH(OH) ₂ (aq)	2.53×10^3	-33.5	28
HCHO(g) ↔ HCH(OH) ₂ (aq)	6.3×10^3	-53.8	29
CH ₃ COCHO(g) ↔ CH ₃ COCH(OH) ₂ (aq)	6.8×10^{3f}		
CH ₃ COCHO(aq) ↔ CH ₃ COCH(OH) ₂ (aq)	2.7×10^3	-30 ^g	9

^a *K*_a = [H⁺][B⁻]/[A⁽¹⁻ⁿ⁾]. ^b At 25 °C and $\mu = 0$. ^c Corrected to $\mu = 0.2$ M using Davies' equation (ref 24). ^d Estimated from $-RT \ln K$ and an assumed value of $\Delta S = 150$ J/(mol·K) (which is typical for a singly charged acid dissociating to produce its doubly charged conjugate base; ref 25a). ^e Dimensionless or M atm⁻¹ (for Henry's low constants). ^f Calculated from $1/K_4$ assuming that *K* for CH₃COCHO(g) ↔ CH₃COCHO(aq) = 2.5; i.e., that the intrinsic Henry's law constant is approximately the same as that for formaldehyde. ^g Estimated from ΔH_{298} for the analogous reaction involving formaldehyde.

biphenol kinetics are observed. For ease of presentation the dehydration and addition reactions will be discussed separately before an overall rate equation is given. Finally the results of the dissociation kinetics and the temperature studies will be presented. For convenience, all the relevant reactions, equilibria, and mass-balance definitions are given now by eq 4, 5, and 6.

Dehydration. Preliminary experiments showed that between pH 4.0 and 7.0, *k*_{obsd} was independent of [MG] ($(0.5-5.0) \times 10^{-3}$ M) but the reaction was catalyzed by S(IV) ($2.50 \times 10^{-3}-1.56 \times 10^{-1}$ M), by phosphate ($5.00 \times 10^{-2}-1.25 \times 10^{-1}$ M total phosphate), and by acetate ($5.00 \times 10^{-2}-2.00 \times 10^{-1}$ M total acetate). There was no direct relationship between *k*_{obsd} and pH at fixed [MG] and [S(IV)]. This behavior is similar to that reported for the dehydration of methylene glycol.¹⁹ In the following reaction sequence we assume that the keto carbonyl of methylglyoxal is unhydrated.



$$[\text{MG}] = [\text{CH}_3\text{COC}^+\text{H}(\text{OH})] + [\text{CH}_3\text{COCH}(\text{OH})_2] + [\text{CH}_3\text{COCHO}] \quad (6a)$$

$$[\text{HAMS}] = [\text{CH}_3\text{COCH}(\text{OH})\text{SO}_3\text{H}] + [\text{CH}_3\text{COCH}(\text{OH})\text{SO}_3^-] + [\text{CH}_3\text{COCH}(\text{O}^-)\text{SO}_3^-] \quad (6b)$$

$$[\text{S(IV)}] = [\text{H}_2\text{O} \cdot \text{SO}_2] + [\text{HSO}_3^-] + [\text{SO}_3^{2-}] \quad (6c)$$

(23) Herbo, C.; Sigalla, J. *Anal. Chim. Acta* **1957**, *17*, 199–207.

(24) Butler, J. N. *Ionic Equilibrium. A Mathematical Approach*; Addison-Wesley: Reading, 1964.

(25) (a) Smith, R. M.; Martell, A. E. *Critical Stability Constants*; Plenum: New York, 1976; Vol. 4. (b) Sillen, G. L.; Martell, A. E. *Stability Constants of Metal-Ion Complexes*; Sp. Publ. 17; Chemical Society: London, 1964.

(26) Potentiometric titration of 0.01 M HAMS in 0.1 M Na₂SO₃ under nitrogen gave *K*_a = 1.72×10^{-11} M at 25 °C and $\mu = 0.3$. Full details will be published elsewhere.

(27) Calculated from the ratio of the effective Henry's law constant *H*^{*} (6.3×10^3 ; ref 29) to the hydration constant, $1/K_4$ (2.53×10^3 ; ref 28).

(28) Bell, R. P. *Adv. Phys. Org. Chem.* **1966**, *4*, 1–29.

(29) Ledbury, W.; Blair, E. W. *J. Chem. Soc.* **1925**, 2832–9.

(30) Hayon, E.; Treinin, A.; Wilf, J. *J. Am. Chem. Soc.* **1972**, *94*, 47–57.

TABLE II: Kinetic Data for the Dehydration of $\text{CH}_3\text{COCH}(\text{OH})_2^a$

pH	buffer	$10^2[\text{A}]^b$, M	$10^4[\text{MG}]$, M	$10^3[\text{S(IV)}]$, M	10^2k_{obsd} , s^{-1}	$10^2k'$, $\text{M}^{-1}\text{s}^{-1}$
7.00	phosphate	3.50	5	5	4.72 ± 0.05	1.19^e
		1.89	5	5	3.12 ± 0.1	
		1.04	5	5	2.27 ± 0.07	
		3.50	5	2.5	4.70 ± 0.1	
7.00	S(IV)	0.19	5	5	1.24 ± 0.01^c	
6.97	S(IV)	1.74	5	44.75^d	1.65 ± 0.03	1.19
6.40	phosphate	8.92	5	5	3.86 ± 0.05	1.18^e
		4.70	5	5	2.62 ± 0.2	
		2.45	5	5	1.90 ± 0.05	
		0.35	5	5	1.18 ± 0.05^c	
6.40	S(IV)	0.35	5	5	1.18 ± 0.05^c	
6.33	S(IV)	4.74	5	64.47^d	1.89 ± 0.03	1.12
6.00	phosphate	13.34	5	5	3.17 ± 0.07	0.86^e
		6.95	5	5	2.14 ± 0.07	
		3.56	5	5	1.44 ± 0.05	
		13.34	5	2.5	3.07 ± 0.2	
		13.34	50	25	3.51 ± 0.01	
6.00	S(IV)	0.43	5	5	0.86 ± 0.1^c	
5.93	S(IV)	6.83	5	78.13^d	1.64 ± 0.02	0.81
5.00	acetate	5.88	2.5	2.5	1.48 ± 0.09	0.63^e
		2.94	2.5	2.5	1.10 ± 0.02	
		1.47	2.5	2.5	0.91 ± 0.03	
		0.74	2.5	2.5	0.72 ± 0.03	
		11.37	2.5	2.5	1.79 ± 0.04	
4.50	acetate	1.42	2.5	2.5	0.75 ± 0.06	0.57^e
		16.13	2.5	2.5	2.33 ± 0.07	0.84^e
4.00	acetate	2.16	2.5	2.5	1.06 ± 0.04	

^aAt 25 °C; $\mu = 0.2$ M. Error limits throughout this work are \pm one standard deviation. ^b $[\text{A}] = [\text{buffer}]_T / (1 + \log^{-1}(\text{pH} - \text{p}K_a))$; ref 15. ^cTaken from the intercept of the phosphate line at the same pH. ^d $[\text{S}_2\text{O}_3^{2-}] < 1\%$ $[\text{S(IV)}]$; ref 30b. ^eCorrection for S(IV) catalysis included (see text).

$[\text{S(IV)}]_0 \gg [\text{MG}]_0$ (the subscript indicates initial concentration), the equilibrium lies far to the right, and the hydration reaction involving k_h in eq 4a has been ignored. This approximation implies that SO_3^{2-} is such a good nucleophile compared to H_2O that under our experimental conditions $k_2[\text{SO}_3^{2-}] \gg k_h[\text{H}_2\text{O}]$. From published polarographic studies⁹ we estimate that $k_h \sim 1 \text{ M}^{-1} \text{ s}^{-1}$ and hence $k_h[\text{H}_2\text{O}] \sim 55 \text{ s}^{-1}$, whereas our kinetic studies (see later) show that $k_2 \sim 10^8 \text{ M}^{-1} \text{ s}^{-1}$ and so $k_2[\text{SO}_3^{2-}] > \sim 10^5 \text{ s}^{-1}$ which justifies our assumption. We also assume that reactions 4b-d and the proton-transfer equilibria of eq 5 are rapid compared to the dehydration step. Then the formation of HAMS as a function of time is given by

$$d[\text{HAMS}]/dt = \frac{k_d[\text{MG}]}{1 + K_d + K_d[\text{H}^+]/K_{a0}} \quad (7a)$$

and

$$[\text{HAMS}] = \frac{(1 - e^{-k_d t}) [\text{MG}]_0}{1 + K_d + K_d[\text{H}^+]/K_{a0}} \quad (7b)$$

where K_d is defined by

$$K_d = k_d/k_h = [\text{CH}_3\text{COCHO}]/[\text{CH}_3\text{COCH}(\text{OH})_2] \quad (7c)$$

This predicts the observed simple first-order kinetics where $k_{\text{obsd}} = k_d$. K_d is the dehydration constant, K_{a0} is the acid dissociation constant defined by eq 5a, and $[\text{MG}]$ is the sum of free aldehyde, hydrated aldehyde, and protonated hydrate shown in eq 6a. The macroscopic dehydration rate constant, k_d , may be written as the sum of several microscopic rate constants¹⁹

$$k_d = k_w + k_H[\text{H}^+] + k_{\text{OH}}[\text{OH}^-] + k_A[\text{A}] + k_B[\text{B}] \quad (8a)$$

where k_w is the intrinsic or "water" rate constant, k_H and k_{OH} are the rate constants associated with specific acid and base catalysis, respectively, and k_A and k_B are the rate constants associated with a general acid-base pair(s) A-B. At constant pH, where $[\text{B}]/[\text{A}] = K_a/[\text{H}^+] = X$, eq 8a simplifies to

$$k_d = k' + (k_A + Xk_B)[\text{A}] \quad (8b)$$

At fixed $[\text{MG}]_0$ and $[\text{S(IV)}]_0$, plots of k_{obsd} vs. $[\text{A}]$ were linear with non-zero intercepts. Values of k_A and k_B were obtained by varying the pH (and thus the buffer ratio, X) and k' was given by the intercept of the straight-line graphs. Since S(IV) was

TABLE III: Rate Constants for Catalyzed Diol Dehydration

A	k_A , $\text{M}^{-1} \text{ s}^{-1}$	k_B , $\text{M}^{-1} \text{ s}^{-1}$
a. Methylglyoxal ^a		
H_2O	$((0.9 \pm 0.3)/55.5) \times 10^{-2}$	$(3.1 \pm 1.4) \times 10^4$
H_2PO_4^-	$(7.7 \pm 0.8) \times 10^{-2}$	$(56.9 \pm 0.8) \times 10^{-2}$
HSO_3^-	$(11.6 \pm 1) \times 10^{-2}$	$(9.2 \pm 1.3) \times 10^{-2}$
CH_3COOH	$(8.6 \pm 0.2) \times 10^{-2}$	$((2.3 \pm 0.1) \times 10^{-2})$
H_3O^+	28 ± 14	$((0.9 \pm 0.3)/55.5) \times 10^{-2}$
b. Formaldehyde ^b		
H_2O	$(0.51/55.5) \times 10^{-2}$	1.6×10^3
H_2PO_4^-	8.8×10^{-2}	39×10^{-2}
HSO_3^-		22×10^{-2}
CH_3COOH	4.3×10^{-2}	2.2×10^{-2}
H_3O^+	2.7	$(0.51/55.5) \times 10^{-2}$

^aAt 25 °C; $\mu = 0.2$ M. ^bReference 19; 25 °C; $\mu = 0.2$ M (?).

always present as a scavenger it was also always present as a catalyst for the dehydration reaction in the acetate and phosphate buffers and so eq 8a contained two k_A and two k_B terms (except when the buffer was $\text{HSO}_3^-/\text{SO}_3^{2-}$). Thus k' derived from the acetate and phosphate buffer experiments included a contribution from $k_{\text{HSO}_3^-}$ and from $k_{\text{SO}_3^{2-}}$, and k' required a correction. The experimental data are summarized in Table II where values of k' have been corrected for the presence of S(IV) by using the experimentally determined values of $k_{\text{HSO}_3^-}$ and $k_{\text{SO}_3^{2-}}$, i.e., $k' = k_w + k_H[\text{H}^+] + k_{\text{OH}}[\text{OH}^-]$. It is assumed that NaCl is catalytically inert. Approximate values of k_H and k_{OH} were obtained by plotting k' vs. $[\text{H}^+]$ which gave k_H (for pH 4.00–5.00) and k_{OH} (for pH 5.97–7.00) from the slope. (Both $[\text{H}^+]$ and $[\text{OH}^-]$ were calculated from the measured pH.) These data were then used to calculate an approximate value for k_w using the average of all the k' data from pH 4.00 to 7.00. It should be noted that these are approximate values only. The "catalytic" rate constants are summarized in Table III and the Brønsted plot for the general bases B is shown in Figure 1. The slope of the least-squares straight line is 0.58 and the coefficient of correlation is 0.994. A plot of $\log k_A$ vs. $\text{p}K_a$ has a slope of -0.34 but shows more scatter (coefficient of correlation = 0.958).

Rate of Formation of HAMS. At low pH, where $\text{H}_2\text{O}\cdot\text{SO}_2$ absorbs intensely,²¹ it was convenient to study the formation reaction with $[\text{MG}]_0 \gg [\text{S(IV)}]_0$. This also made k_{obsd} insensitive to slow S(IV) oxidation. From pH 0.7 to pH 2.0 the formation

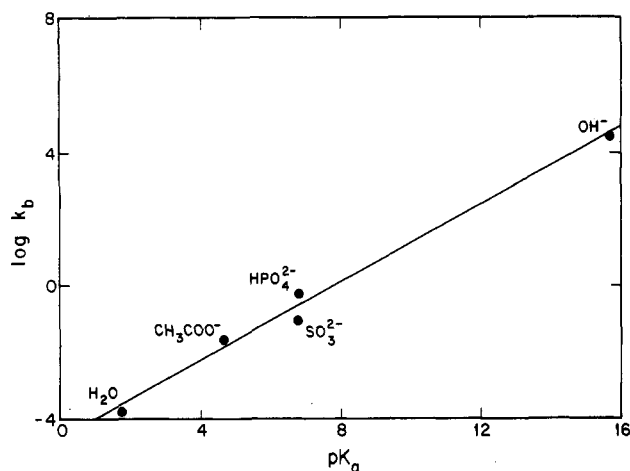


Figure 1. Brønsted plot for the general base-catalyzed dehydration of CH₃COCH(OH)₂. The slope of the least-squares line is 0.58.

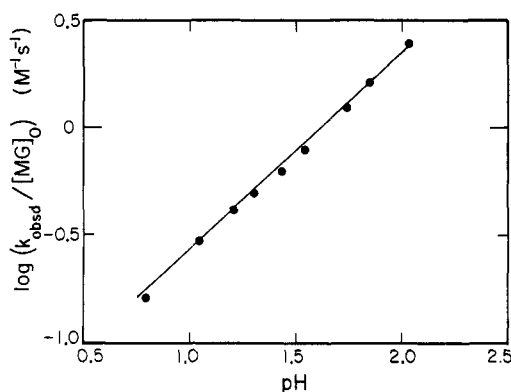


Figure 2. Pseudo-second-order rate constants for the formation of hydroxyacetylmethanesulfonate as a function of pH. The straight line is a least-squares fit of the data.

TABLE IV: Kinetic Data for the Rate of Formation of HAMS^a

pH	10 ² [MG] ₀ , M	10 ³ [S(IV)] ₀ , M	10 ³ k _{obsd} /[MG] ₀ , M ⁻¹ s ⁻¹
0.78	0.5–1.0	0.5–1.0	1.61 ± 0.03
1.04	0.5–1.0	0.5–1.0	2.93 ± 0.02
1.21	0.5–1.0	0.5–1.0	4.17 ± 0.13
1.31	0.5–1.0	0.5–1.0	4.93 ± 0.34
1.43	0.5–1.0	0.5–1.0	6.19 ± 0.39
1.54	0.125–1.0	0.25–1.0	7.87 ± 0.30
1.74	0.5–1.0	0.5	12.26 ± 0.09
1.85	0.5–1.0	0.5	16.06 ± 0.58
2.03	0.5–1.0	0.5	24.13 ± 1.10

^aAt 25 °C; μ = 0.2 M; [MG]₀/[S(IV)]₀ ≥ 10.

reaction showed simple pseudo-first-order kinetics and k_{obsd} was independent of [S(IV)]₀ ((0.50–1.00) × 10⁻³ M) but was dependent on [MG]₀ ((0.50–1.00) × 10⁻² M) with [MG]₀ ≥ 10[S(IV)]₀. Plots of k_{obsd} vs. [MG]₀ were linear and passed through the origin; i.e., the y intercept was 0 ± 2σ. The calculated pseudo-second-order rate constants, $k_{\text{obsd}}/[MG]_0$, are given in Table IV, and they are plotted in Figure 2 which shows the linear increase of $\log(k_{\text{obsd}}/[MG]_0)$ with pH.

If we assume that the diol dehydration equilibrium (eq 4a) is established rapidly in this pH region and that the simple proton-transfer reactions (eq 5) are rapid, then eq 4 leads to the following rate law for the loss of S(IV) (and the formation of HAMS)

$$\frac{-d[S(IV)]}{dt} = \left(\frac{k_0 \alpha_1 [H^+]}{K_{a0}} + k_1 \alpha_1 + k_2 \alpha_2 \right) [S(IV)] \frac{[MG]_0 K_d}{1 + K_d + K_d [H^+] / K_{a0}} \quad (9)$$

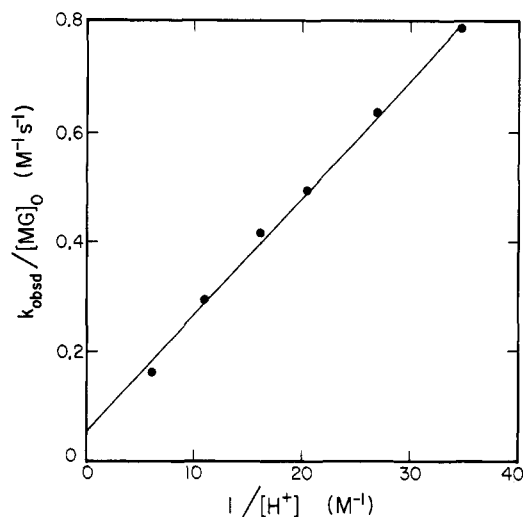


Figure 3. Rate of formation of hydroxyacetylmethanesulfonate at low pH plotted to obtain k_1 (from slope/ $K_{a1}K_d$) and k_0/K_{a0} (from intercept/ $K_{a1}K_d$). The straight line is a linear least-squares fit of the data.

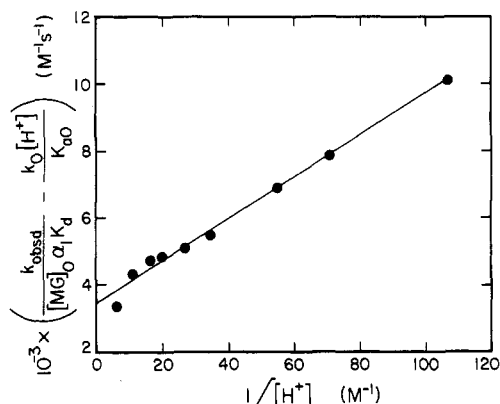


Figure 4. Linear plot of all the rate of formation data (for hydroxyacetylmethanesulfonate) used to obtain k_2 (from slope/ K_{a2}) and a second estimate of k_1 (from the intercept). The straight line is the linear least-squares fit of the data.

in which the pseudo-first-order approximation $[MG] \sim [MG]_0$ has been made, and where α_1 and α_2 , the fraction of HSO₃⁻ and SO₃²⁻ respectively, are given by eq 10a and 10b:

$$\alpha_1 = \frac{K_{a1}[H^+]}{[H^+]^2 + K_{a1}[H^+] + K_{a1}K_{a2}} \quad (10a)$$

$$\alpha_2 = \alpha_1 K_{a2} / [H^+] \quad (10b)$$

The magnitude of K_{a0} is unknown, but it is almost certainly much greater than $K_d[H^+]$ (K_{a0} for benzaldehyde is $\sim 10^7$ M)³¹ and $K_d \ll 1$ so that eq 9 may be simplified and written in terms of k_{obsd} :

$$\frac{k_{\text{obsd}}}{[MG]_0} = \left(\frac{k_0 \alpha_1 [H^+]}{K_{a0}} + k_1 \alpha_1 + k_2 \alpha_2 \right) K_d \quad (11a)$$

At pH ≤ 1.5, $\alpha_1 \sim K_{a1}/[H^+]$ and $\alpha_2 \sim 0$ and so eq 11a becomes eq 11b. The linear plot of $k_{\text{obsd}}/[MG]_0$ vs. $1/[H^+]$ is shown in

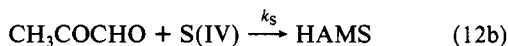
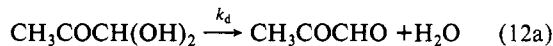
$$k_{\text{obsd}}/[MG]_0 = k_0 K_{a1} K_d / K_{a0} + k_1 K_{a1} K_d / [H^+] \quad (11b)$$

Figure 3. The value of $k_0/K_{a0} = (8.25 \pm 2.1) \times 10^3$ M⁻² s⁻¹ is given by the intercept/ $K_{a1}K_d$, and $k_1 = (3.44 \pm 0.1) \times 10^3$ M⁻¹ s⁻¹ is given by slope/ $K_{a1}K_d$. Equation 11a may be rearranged to obtain k_2 and a second estimate of k_1 (using all the experimental data):

$$\frac{k_{\text{obsd}}}{[MG]_0 \alpha_1 K_d} - \frac{k_0}{K_{a0}} [H^+] = k_1 + \frac{k_2 K_{a2}}{[H^+]} \quad (11c)$$

The linear plot of the left side of eq 11c vs. $1/[H^+]$ is shown in Figure 4: slope/ $K_{a2} = k_2 = (3.66 \pm 0.14) \times 10^8 \text{ M}^{-1} \text{ s}^{-1}$ and intercept = $k_1 = (3.45 \pm 0.12) \times 10^3 \text{ M}^{-1} \text{ s}^{-1}$ (in good agreement with the low-pH data). It was not possible to extend the formation studies to higher pH where the approximation $k_0\alpha_1[H^+]/K_{a0} \sim 0$ would be valid because of the complications introduced by the appearance of biexponential kinetics at $\text{pH} \geq 2.5$.

Overall Rate Equation. Between about $\text{pH} 2.5$ and 3.5 the kinetics of both the dehydration reaction (with $[MG] \ll [S(IV)]$) and the formation reaction (with $[MG] \gg [S(IV)]$) were complicated by the appearance of a second reaction. The second reaction was not due to the chloroacetate buffer used in this pH region because unbuffered solutions containing only NaCl as the inert electrolyte showed the same behavior. Under the conditions of the dehydration experiments, there are two consecutive "irreversible" reactions represented by eq 12a and 12b since the equilibrium lies far to the right



where the rate constant k_s for the S(IV) reaction is given by eq 12c (cf. eq 9):

$$k_s = ((k_0\alpha_1[H^+]/K_{a0}) + k_1\alpha_1 + k_2\alpha_2)[S(IV)] \quad (12c)$$

Since $[S(IV)] \gg [MG]$, eq 12a and 12b are consecutive (pseudo) first-order reactions and substitution into the integrated expression^{20c} for this type of reaction gives

$$[\text{HAMS}] = \left\{ 1 + \frac{1}{k_d - k_s} (k_s e^{-k_d t} - k_d e^{-k_s t}) \right\} [\text{CH}_3\text{COCH}(\text{OH})_2]_0 \quad (13a)$$

or

$$[\text{HAMS}] = \left\{ 1 + \frac{1}{k_d - k_s} (k_s e^{-k_d t} - k_d e^{-k_s t}) \right\} \frac{[\text{MG}]_0}{1 + K_d + K_d[H^+]/K_{a0}} \quad (13b)$$

When the rates of dehydration and addition are approximately equal, i.e., when $k_d \sim k_s$, then eq 13 predicts that biexponential kinetics would be observed but when $k_s \gg k_d$ then, as we would expect, eq 13b reduces to eq 7b derived for the dehydration reaction. Conversely when $k_d \gg k_s$ eq 13b reduces to eq 14a.

$$[\text{HAMS}] = \frac{(1 - e^{-k_s t}) [\text{MG}]_0}{1 + K_d + K_d[H^+]/K_{a0}} \quad (14a)$$

This is the same as the integrated form of the rate expression for the formation of HAMS from MG and excess S(IV), i.e., the integrated form of eq 9 but with $[S(IV)] \sim [S(IV)]_0$:

$$-d[S(IV)]/dt = d[\text{HAMS}]/dt = k_s[\text{CH}_3\text{COCHO}] = k_s([\text{CH}_3\text{COCH}(\text{OH})_2]_0 - [\text{HAMS}]) \quad (14b)$$

and

$$[\text{HAMS}] = (1 - e^{-k_s t}) [\text{CH}_3\text{COCH}(\text{OH})_2]_0 \quad (14c)$$

Since both k_d and k_s include terms involving $[S(IV)]$, the observed macroscopic rate constants $k_{\text{obsd}1}$ and $k_{\text{obsd}2}$ both increase with $[S(IV)]$ and plots of both $k_{\text{obsd}1}$ and $k_{\text{obsd}2}$ vs. $[S(IV)]$ were linear. However, it was difficult to obtain reproducible results at $\text{pH} \leq 3.5$ because of the small absorbance changes which were superimposed on the large background signal (see Experimental Section) and consequently quantitative results for the dehydration experiments in this pH region are not reported. Qualitatively, the observed rate constants were consistent with those obtained at higher pH.

Rate of Dissociation of HAMS. The rate of dissociation of HAMS in the presence of I_2 was independent of $[I_2]$ ($(0.37-1.00) \times 10^{-3} \text{ M}$), $[I^-]$ ($(0-1.00) \times 10^{-4} \text{ M}$ added I^-), and $[\text{HAMS}]_0$

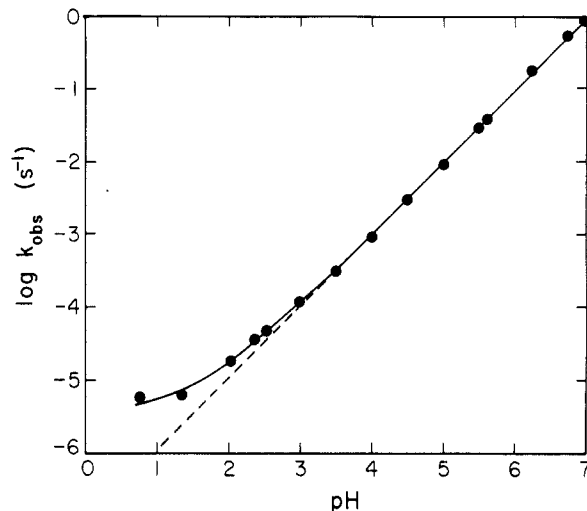


Figure 5. Rate of dissociation of hydroxyacetylmethanesulfonate as a function of pH. The solid line is calculated by using eq 15 and the broken line is an extension of a least-squares line (of unit slope) for $\text{pH} > 3$.

TABLE V: Kinetic Data for the Dissociation of HAMS^a

pH	$10^5[\text{HAMS}]_0, \text{ M}$	$10^4[I_2]_0, \text{ M}$	$k_{\text{obsd}}, \text{ s}^{-1}$
0.77	8.6	7.5	$(5.78 \pm 2.1) \times 10^{-6}$
1.35	16.0	10.0	6.33×10^{-6}
2.03	16.0	10.0	$(1.81 \pm 0.10) \times 10^{-5}$
2.36	16.3	10.0	3.49×10^{-5}
2.52	16.0	10.0	$(4.78 \pm 0.30) \times 10^{-5}$
3.00	8.4	7.5	$(1.24 \pm 0.03) \times 10^{-4}$
3.00 ^b	7.8	7.6	1.26×10^{-4}
3.50	8.5	7.5	3.15×10^{-4}
4.00	8.5	7.5	$(9.40 \pm 0.63) \times 10^{-4}$
4.50	8.4	7.4	$(3.09 \pm 0.09) \times 10^{-3}$
5.00	11.7	5.0	$(9.26 \pm 0.35) \times 10^{-3}$
5.00	5.8	5.0	8.92×10^{-3}
5.00	15.9	10.0	$(9.30 \pm 0.47) \times 10^{-3}$
5.50	8.5	7.5	$(2.86 \pm 0.06) \times 10^{-2}$
5.61 ^c	5.1	3.7	$(3.95 \pm 0.03) \times 10^{-2}$
6.24 ^c	5.2	3.9	$(1.74 \pm 0.03) \times 10^{-1}$
6.72 ^c	5.1	3.8	$(5.43 \pm 0.29) \times 10^{-1}$
6.98 ^c	5.1	3.7	$(8.58 \pm 0.10) \times 10^{-1}$

^a At 25 °C; $\mu = 0.2 \text{ M}$. ^b By conventional UV/vis spectrophotometry at 458 nm. ^c By stopped-flow spectrophotometry at 449 nm.

($(0.51-2.34) \times 10^{-4} \text{ M}$) with $[I_2]_0 \geq 5[\text{HAMS}]_0$, but k_{obsd} was proportional to $1/[H^+]$ (see Figure 5). The experimental data are summarized in Table V. Since $[I_2]$ was always in excess of $[\text{HAMS}]$ the formation reaction, i.e., terms involving k_0, k_1 , and k_2 , can be ignored and eq 4 leads to eq 15 for the rate of release of S(IV) (and consequently the rate of production of I^- ; see Experimental Section).

$$\frac{d[S(IV)]}{dt} = \left(k_{-0}[H^+] + k_{-1} + \frac{k_{-2}K_{a3}}{[H^+]} \right) \frac{K_{a4}[H^+][\text{HAMS}]}{[H^+]^2 + K_{a4}[H^+] + K_{a3}K_{a4}} \quad (15)$$

Although α -hydroxysulfonic acids are generally considered to be strong acids, little consistent quantitative data are available. For example, the $\text{p}K_a$ of α -hydroxybenzenesulfonic acid has been estimated¹³ to be as low as -8.6 but a qualitative titration³ yielded $\text{p}K_a \sim 0.7$. If we assume that the $\text{p}K_a$ of α -hydroxyacetylmethanesulfonic acid lies between these two extremes at $\text{p}K_a \sim -3$, then $K_{a4} = 10^3$ and at $\text{pH} < 3$, $[H^+]^2$ and $K_{a4}K_{a3} \ll K_a[H^+]$ and eq 15 may be written as

$$k_{\text{obsd}} = k_{-0}[H^+] + k_{-1} + \frac{k_{-2}K_{a3}}{[H^+]} \quad (16)$$

The plot of k_{obsd} vs. $1/[H^+]$ ($0.88 \leq \text{pH} < 3$) is linear (see Figure

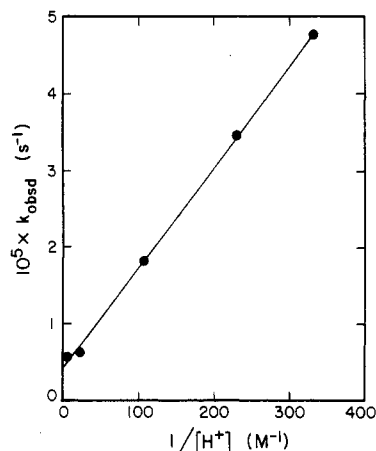


Figure 6. Rate of dissociation of hydroxyacetylmesulfonate at low pH plotted to obtain k_{-1} (from the intercept) and k_{-2} (from slope/ K_{a3}). The straight line is a least-squares fit of the data.

6) which implies that $k_{-3}[H^+] \ll k_{-1}$. Taking the intercept on the y axis to be equal to k_{-1} , and $k_{-2} = \text{slope}/K_{a3}$ we calculate that $k_{-0} \ll 2.5 \times 10^{-5} \text{ s}^{-1}$, $k_{-1} = (4.18 \pm 0.47) \times 10^{-6} \text{ s}^{-1}$, and $k_{-2} = (6.79 \pm 0.13) \times 10^3 \text{ s}^{-1}$. Inspection of Figure 5 shows that $k_{-0}[H^+]$ must be small even at pH 0.7 because, although the line shows some curvature, there is no indication of an increase in rate as the pH drops further. This is in contrast to the analogous pH profile for *p*-methoxyacetophenone bisulfite¹³ which shows a pronounced minimum in the curve at pH 2.5. Since $k_2 K_{a3}/[H^+] \gg k_{-0}[H^+]$ and k_{-1} at pH >3.0, a plot of $\log k_{\text{obsd}}$ vs. pH should be linear with unit slope and an intercept of $\log k_{-2} K_{a3}$ (Figure 5). The slope of the straight line is 0.99 ± 0.01 and $(\log^{-1}(\text{intercept}))/K_{a3} = (6.00 \pm 0.65) \times 10^3 \text{ s}^{-1}$. The average value of k_{-2} is thus $(6.40 \pm 0.56) \times 10^3 \text{ s}^{-1}$.

Temperature Studies. The dependence of k_1 and k_2 on temperature from 15.0 to 40.0 °C was determined at pH 1.05 and 1.30 for k_1 , and at pH 1.76 for k_2 . The slope of a plot of $k_{\text{obsd}}/[\text{MG}]_0$ vs. $1/[H^+]$ gave k_1 at each temperature (eq 11b) and k_2 was calculated from eq 11a assuming that $k_0[H^+]/K_{a0}$ is a constant equal to $1.43 \times 10^2 \text{ M}^{-1} \text{ s}^{-1}$. K_{a1} , K_{a2} , and K_d were corrected for temperature by using the integrated van't Hoff equation and the enthalpies listed in Table I. Graphs of $\ln(k_1/T)$ vs. $1/T$ and $\ln(k_2/T)$ vs. $1/T$ were linear, as expected from the transition-state theory, with $\Delta H^\ddagger = (-\text{slope}/T)$ and $\Delta S^\ddagger = ((\text{intercept} - \ln \kappa/h)R)$; where κ is Boltzman's constant, $1.380 \times 10^{-23} \text{ J/K}$; h is Planck's constant, $6.626 \times 10^{-34} \text{ J s}$; and R is the gas constant, $8.314 \text{ J/(K}\cdot\text{mol)}$. The calculated values of ΔH^\ddagger and ΔS^\ddagger are given in Table VI.

The dependence of k_{-1} on temperature at pH 2.40 was determined from 25.0 to 47.9 °C because at low temperature the reaction became inconveniently slow. The temperature range for determining the effect of temperature on k_{-2} was 15.0–40.0 °C at pH 4.54. At this pH, $k_{-2} K_{a3}/[H^+] \gg k_{-0}[H^+]$, k_{-1} , and eq 16 becomes eq 17 which was used to calculate k_{-2} . K_{a3} was corrected

$$k_{\text{obsd}} = k_{-2} K_{a3}/[H^+] \quad (17)$$

for temperature and k_{-1} was calculated from eq 16 assuming that $k_{-3}[H^+] = 0$. An extrapolated value for k_{-2} at 47.9 °C was included in the latter calculation. Linear plots of $\ln(k/T)$ vs. $1/T$ yielded the activation parameters summarized in Table VI. Linear graphs of $R \ln K_1$ and $R \ln K_2$ vs. $1/T$, where $K_1 = k_1/k_{-1}$ and $K_2 = k_2/k_{-2}$, gave ΔH_{298} and ΔS_{298} for eq 4c and 4d (Table VI).

Discussion

Within the limited range of catalysts and catalyst concentrations studied here, the dehydration of the diol of methylglyoxal is clearly the rate-determining step in the formation of HAMS at pH ≥ 4.0 and the rate of dehydration is subject to acid and base catalysis. A comparison of the rate constants k_A and k_B found for CH₃C(OCH(OH))₂ with those reported¹⁹ for HCH(OH)₂ (Table III)

TABLE VI: Thermodynamic Parameters for Some Aldehyde-S(IV) Systems

reaction path	ΔH^\ddagger ^b	ΔS^\ddagger ^c	ΔH_{298} ^b	ΔS_{298} ^c
a. Methylglyoxal ^a				
k_1	29.0 ± 3.2	-77.7 ± 10.8		
k_2	18.2 ± 4.4	-22.6 ± 14.4		
k_{-1}	81.7 ± 11.5	-61.6 ± 37.3		
k_{-2}	70.6 ± 0.7	$+61.9 \pm 2.4$		
K_1			-54.5 ± 0.9	-27.0 ± 1.3
K_2			-52.7 ± 0.7	-85.7 ± 0.5
b. Formaldehyde ^d				
k_1	24.9	-108.0		
k_2	20.4	-31.7		
K_1 ^e			-54.6 ± 1.1	-57.6 ± 3.7
c. Benzaldehyde ^f				
k_1	36.6	-142		
k_2	36.0	-58.1		
K_1			-64.6	-146

^aThis work. The cumulative error of all the corrections (see text) led to larger than normal scatter and large uncertainties in the calculated values of ΔH and ΔS . ^bUnits are kJ/mol. ^cUnits are J/(mol·K). ^dReference 2. ^eReference 11e. ^fReference 3.

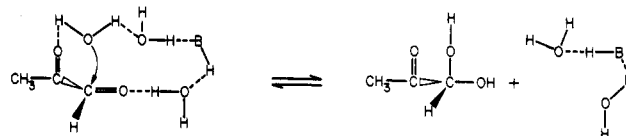


Figure 7. The acid (B-H) catalyzed hydration and dehydration of methylglyoxal may involve hydrogen bonding of water to the keto carbonyl group.

shows that while there is no major difference in the effect of the catalysts on either diol, the catalysts have a stronger effect on methylglyoxal dehydration. Bell and Evans¹⁹ were unable to detect catalysis by HSO₃⁻ but we find that its catalytic effect on CH₃COCH(OH)₂ dehydration is quite marked. The anionic acids such as H₂PO₄⁻, H₂PO₃⁻, and H₂AsO₄⁻ are effective catalysts for methylene glycol dehydration and so our observation that HSO₃⁻ is a catalyst is not entirely unexpected. The catalytic effect of HSO₃⁻ may be associated with the formation of a hydrogen-bonded intermediate involving the keto carbonyl group of hydrated methylglyoxal—a pathway which would not be available to methylene glycol. A possible structure for such an intermediate is given in Figure 7. The rapid hydration of neutral pyruvic acid, CH₃COCOOH (but not its conjugate base CH₃COCOO⁻ or CH₃C(OH)₂COO⁻) has been suggested^{28,32} to occur through an intramolecular catalysis by the carboxyl group. Our data are consistent with the proposal²⁸ that catalysis of the aldehyde dehydration reaction occurs through a concerted mechanism involving several molecules of water.

The extensive set of rate constants compiled by Bell and Evans¹⁹ shows that in general k_A decreases with an increase in the pK_a of the catalyst while k_B increases. We observe the same trend (for the conjugate bases at least; see Figure 1) but over a more limited range of catalysts (Table III). The coefficients (i.e., the magnitude of the slope) of the Brønsted plots obtained for the base catalysts (0.58) and for the acid catalysts (0.34) are comparable to the analogous coefficients reported²⁸ for the catalyzed dehydration of formaldehyde (0.45 and 0.23, respectively) and for the dehydration of acetaldehyde (0.45 and 0.54, respectively). The strong correlation of k_A and k_B with the pK_a of the catalyst in Brønsted plots has been discussed in detail by Bell and Evans¹⁹ and by Bell.²⁸

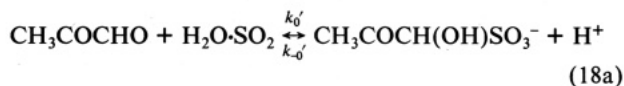
There is insufficient information to make a direct comparison of our dehydration rate constants with those of Wasa and Musha,⁹ determined polarographically, but they report $k_d = 2 \times 10^{-2} \text{ s}^{-1}$

(32) (a) Eigen, M.; Kustin, K.; Strehlow, H. *Z. Phys. Chem. (Frankfurt/Main)* **1962**, *31*, 140–3. (b) Strehlow, H. *Z. Elektrochem.* **1962**, *66*, 392–6.

at pH 7 (and unspecified μ) which is consistent with our results which are in the range $(1.24\text{--}4.72) \times 10^{-2} \text{ s}^{-1}$ at pH 7. At about pH 2.5–3.5, where biexponential kinetics are observed, we propose that the rate of dehydration is catalyzed sufficiently by the increased $[\text{H}^+]$ to become comparable to the rate of addition of S(IV) to the free aldehyde so that both reactions become experimentally observable. By setting the rate of dehydration (eq 7a) equal to the rate of S(IV) addition (eq 9) it is possible to construct a pH–S(IV) profile which divides the region where dehydration is rate determining from that where S(IV) addition is rate determining. Although the edges of the “envelope” in Figure 8 will be blurred by the presence of catalysts, it demonstrates that under the conditions where we observed biexponential kinetics (pH 2.5–3.5, S(IV) 10^{-4} – 10^{-2} M) we were indeed working in the boundary area. The boundary line was drawn assuming no general catalysts except S(IV) are present. This behavior has recently been postulated³³ to occur for formaldehyde but this is the first experimental evidence for a change in the rate-determining step.

At pH ≤ 2 , where dehydration is much faster than S(IV) addition, the observed kinetics are due solely to the reaction of CH_3COCHO with S(IV). The mechanism is similar to that proposed for the analogous benzaldehyde³ and formaldehyde² systems. One difference, however, is that no reaction between $\text{HC}^+\text{H}(\text{OH})$ and HSO_3^- , i.e., the equivalent of eq 4b, was proposed² for formaldehyde. Evidence for this reaction comes from a nonzero intercept in the $k_{\text{obsd}}/[\text{RCHO}]_0$ vs. $1/[\text{H}^+]$ plot at low pH, e.g., Figure 3, but the small intercept $((3.30 \pm 0.52) \times 10^{-3} \text{ M}^{-1} \text{ s}^{-1})$ was considered to be insignificant in the case of formaldehyde.² If the intercept is in fact real then we have the following series for k_0/K_{a0} : CH_3COCHO $((8.2 \pm 2.1) \times 10^3 \text{ M}^{-2} \text{ s}^{-1}) > \text{HCHO}$ $((3.6 \pm 0.6) \times 10^2 \text{ M}^{-2} \text{ s}^{-1}) > \text{C}_6\text{H}_5\text{CHO}$ $((2.5 \pm 1.5) \text{ M}^{-2} \text{ s}^{-1})$.

It should be noted that the kinetic evidence for reaction 4b is ambiguous since it cannot be used to distinguish this pathway involving a carbocation and HSO_3^- from one involving the free aldehyde and $\text{H}_2\text{O}\cdot\text{SO}_2$. If the latter occurs then eq 4b and 5a are replaced by eq 18a and 18b. The expression for k_{obsd} becomes



$$\alpha_0 = \alpha_1[\text{H}^+]/K_{a1} \quad (18b)$$

$$k_{\text{obsd}} = k_0'K_d + \frac{k_1K_{a1}K_d}{[\text{H}^+]} \quad (18c)$$

eq 18c at low pH when $\alpha_0 \sim 1$, and the magnitude of the intercept of a plot of k_{obsd} vs. $1/[\text{H}^+]$ would then be interpreted as being a measure of k_0' ($= (5.1 \pm 1.3) \times 10^{-2} \text{ M}^{-1} \text{ s}^{-1}$) instead of k_0/K_{a0} . However, $\text{H}_2\text{O}\cdot\text{SO}_2$ is unlikely to be a strong nucleophile and Young and Jencks¹³ have argued in favor of a pathway involving a carbocation at low pH in the dissociation of the *p*-methoxybenzaldehyde–S(IV) adduct.

Our kinetic data confirm that SO_3^{2-} reacts much more rapidly with aldehydes than does HSO_3^- (or $\text{H}_2\text{O}\cdot\text{SO}_2$): k_2 $((3.68 \pm 0.14) \times 10^8 \text{ M}^{-1} \text{ s}^{-1}) \gg k_1$ $((3.43 \pm 0.11) \times 10^3 \text{ M}^{-1} \text{ s}^{-1}) (\gg k_0'$ $((5.1 \pm 1.3) \times 10^{-2} \text{ M}^{-1} \text{ s}^{-1}))$. The rate of reaction of SO_3^{2-} with methylglyoxal is the fastest yet reported for the reaction of SO_3^{2-} with any aldehyde. The ratio k_2/k_1 for methylglyoxal, formaldehyde, and benzaldehyde is 1.14×10^5 , 3.14×10^4 , and 3.02×10^4 , respectively. The ratio appears to be anomalously high for methylglyoxal but it is not clear why.

(33) Olson, T. M.; Hoffmann, M. R. *Atmos. Environ.* **1986**, *20*, 2277–8.

(34) Munger, J. W.; Jacob, D. J.; Hoffmann, M. R. *J. Atmos. Chem.* **1984**, *1*, 335–50.

(35) Perrin, D. D.; Dempsey, B.; Serjeant, E. P. *pK_a Prediction for Organic Acids and Bases*; Chapman and Hall: London, 1981.

(36) Grosjean, D. *Environ. Sci. Technol.* **1982**, *16*, 254–62.

(37) Blackadder, D. A.; Hinshelwood, C. *J. Chem. Soc.* **1958**, 2720–7.

(38) Preliminary results obtained at pH 4.31 and $\mu = 0.2 \text{ M}$ (NaCl) by the method described in ref 11e. Full details will be published elsewhere.

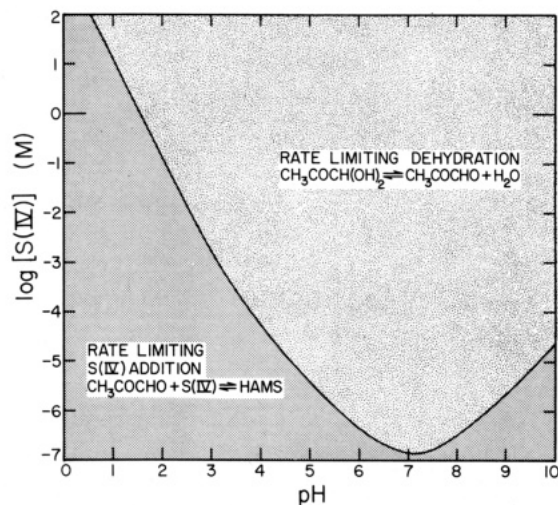


Figure 8. Rate of formation of hydroxyacetylmethanesulfonate determined by either rate-limiting S(IV) addition or rate-limiting dehydration depending on pH and $[\text{S(IV)}]$. The boundary line between the two regions is calculated by equation eq 7 with eq 9 assuming that S(IV) is the only general acid/base catalyst present.

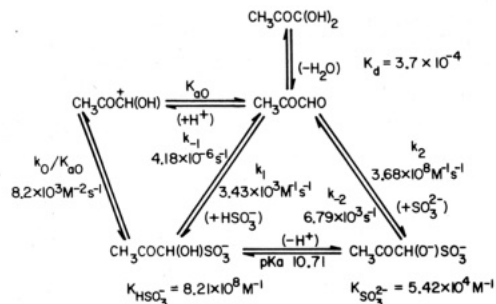


Figure 9. A summary of rate and equilibrium constants for the methylglyoxal–S(IV) system. The stability constants K_1 and K_2 are defined in Table VII.

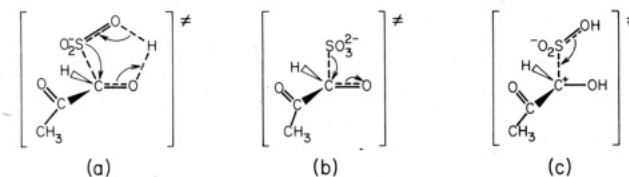


Figure 10. The high entropy of activation, ΔS^\ddagger , of the pathways involving HSO_3^- may be associated with the formation of a cyclic intermediate (a) whereas reactions involving SO_3^{2-} (b) and the postulated carbocation (c) would not involve cyclic species.

The dissociation of HAMS occurs by two major pathways with the expulsion of SO_3^{2-} ($k_{-2} = (6.79 \pm 0.13) \times 10^3 \text{ s}^{-1}$) being much more rapid than the expulsion of HSO_3^- ($k_{-1} = (4.18 \pm 0.47) \times 10^6 \text{ s}^{-1}$). The large difference between k_{-2} and k_{-1} must be at least partly due to the charge difference between $\text{CH}_3\text{COCH}(\text{O}^-)\text{SO}_3^-$ and $\text{CH}_3\text{COCH}(\text{OH})\text{SO}_3^-$ but it may also reflect structural features in the transition-state complex (see later).

The ratio of k_1/k_{-1} and k_2/k_{-2} gives the corresponding stability constant for reactions 4c and 4d, respectively: $K_1 = (8.21 \pm 1.2) \times 10^8 \text{ M}^{-1}$, $K_2 = (5.42 \pm 0.72) \times 10^4 \text{ M}^{-1}$. It can be seen that, although $\text{CH}_3\text{COCH}(\text{OH})\text{SO}_3^-$ is the thermodynamically favorable product ($K_1 \gg K_2$), it is mainly formed via the less thermodynamically stable doubly charged anion, $\text{CH}_3\text{COCH}(\text{O}^-)\text{SO}_3^-$, ($k_2 \gg k_1$) which then rapidly acquires a proton to give HAMS. This is made clear in Figure 9 which summarizes the thermodynamic and kinetic data for the methylglyoxal–S(IV) system.

The thermodynamic activation parameters ΔH^\ddagger and ΔS^\ddagger (Table VI) may indicate why the kinetic behavior of SO_3^{2-} and HSO_3^- should be so different. Although $\Delta H^\ddagger_{k_2}$ is less than $\Delta H^\ddagger_{k_1}$, the major influence on the rate constant comes from ΔS^\ddagger which is

TABLE VII: A Comparison of Some Aldehyde-S(IV) Equilibrium and Rate Constant Data^a

R-CHO	σ^{*b}	$k_1, M^{-1} s^{-1}$	$k_2, M^{-1} s^{-1}$	K_1^n, M^{-1}	K_2^n, M^{-1}	K_d	k_{-1}, s^{-1}	k_{-2}, s^{-1}
CCl ₃ -	2.65					3.6×10^{-5c}		
CH ₃ CO-	1.81	3.45×10^3	3.66×10^8	8.21×10^8	5.42×10^4	3.7×10^{-4d}	4.18×10^{-6}	6.40×10^3
C ₆ H ₅ -	0.75	0.71 ^e	2.2×10^{4e}	4.81×10^{3e}	1.2×10^{2f}		3.7×10^{-5g}	1.8×10^{2g}
H-	0.49	7.9×10^{2h}	2.5×10^{7h}	6.57×10^{9i}	2.2×10^{5j}	5.5×10^{-4c}	2.2×10^{-4f}	4.3×10^{1j}
CH ₃ -	0.00			6.8×10^{5k}		0.65 ^c		
<i>i</i> -Pr-	-0.19		1.4×10^{4m}	4.8×10^{4m}		2.3 ^c		

^a At 25 °C; μ variable (see original reference). Some data are not self-consistent. ^b Reference 35 ^c Reference 28. ^d Reference 9. ^e Reference 3. ^f K_d assumed to be ≥ 10 . ^g Calculated from $K = k_{\text{forward}}/k_{\text{reverse}}$. ^h Reference 12c. ⁱ Reference 2. ^j Reference 11e. ^k Reference 11a. ^l Reference 38. ^m Reference 14. ⁿ $K_1 = [R-CH(OH)SO_3^-]/([R-CHO][HSO_3^-])$ and $K_2 = [R-CH(O^-)SO_3^-]/([R-CHO][SO_3^{2-}])$.

much more positive for SO_3^{2-} than for HSO_3^- : $\Delta S^*_{k_2} = -22.6 \pm 14.4$ J/(mol·K), while $\Delta S^*_{k_1} = -77.7 \pm 10.8$ J/(mol·K). This observation could be explained by the proposal² that the transition state involving HSO_3^- (k_1) involves a highly ordered cyclic intermediate whereas that involving SO_3^{2-} (k_2) does not (see Figure 10). However, a cyclic intermediate is not the only explanation. For example, an alternative explanation could invoke a structured proton-catalyzed pathway for SO_3^{2-} addition which would be kinetically indistinguishable. The comparable thermodynamic data for formaldehyde and benzaldehyde are also given in Table VI. The activation parameters for the dissociation reaction show the same features; i.e., the relative magnitude of the rate constant is largely determined by ΔS^* which is more positive for k_{-2} than for k_{-1} . The doubly charged anion $CH_3COCH(O^-)SO_3^-$ in fact appears to have a positive ΔS^* for the path involving elimination of SO_3^{2-} .

ΔH_{298} and ΔS_{298} for eq 4b and 4c are compared to those for benzaldehyde and formaldehyde in Table VI where the entropy term is again seen to be important: while ΔH_{298} (for K_1) is approximately the same for methylglyoxal, formaldehyde, and benzaldehyde, ΔS_{298} becomes progressively more negative in the order methylglyoxal > formaldehyde > benzaldehyde.

We have assumed that addition reactions occur only at the aldehyde carbonyl and not at the ketone carbonyl site in $CH_3C(O)CHO$. This assumption is based on the fact that aldehydes are well-known to be generally more reactive than ketones both thermodynamically^{39a} and kinetically.^{39b} Elemental and chemical analysis of the adduct prepared during the course of this work supports the assumption since we found only one mole of S(IV) per mole of aldehyde.⁴⁰

Since k_1 and particularly k_2 are so large for methylglyoxal it is possible that mass transport could become the rate-limiting step for the formation of HAMS in naturally occurring water droplets if dehydration of the diol is strongly catalyzed, but it is difficult to test this idea because many assumptions need to be made (droplet size, ionic strength, temperature, and particularly the nature and concentration of catalysts). However, it is possible to compare the rate of S(IV) scavenging by methylglyoxal with the rate of S(IV) scavenging by formaldehyde under conditions where mass transport and dehydration are unlikely to become rate-limiting. If we assume the following partial pressures for gaseous species in an open system: $P_{SO_2} = 20$ ppbv, $P_{HCHO} = 5$ ppbv, $P_{MG} = 1$ ppbv, then at pH 3 and 25 °C the rate of formation of hydroxymethanesulfonate is 5.38×10^{-8} M h⁻¹ while that of hydroxyacetylmethanesulfonate is found to be 2.19×10^{-7} M h⁻¹ by using eq 9 and the appropriate Henry's law relationships. This is 4 times greater than the rate of formation of hydroxymethanesulfonate. ($P_{SO_2} = 20$ ppbv is equivalent to 4×10^{-7} M S(IV) and thus at pH 3 the rate of the S(IV) addition reaction is rate-determining (see Figure 8). $P_{MG} = 1$ ppbv is equivalent to $6.83 \mu\text{M}$ MG in the aqueous phase which is the same order of

magnitude as [MG] found in fog, mist, and rain water.⁸)

The potential of methylglyoxal as a S(IV) reservoir compared to formaldehyde and benzaldehyde may be estimated by calculating the equilibrium total $[S(IV)]_T$ for each aldehyde considered separately in an open system.³⁴

$$[S(IV)]_T = [S(IV)] + [RCH(OH)SO_3^-] + [RCH(O^-)SO_3^-] + [RCH(OH)SO_3H] \quad (19a)$$

At pH 3, eq 19a is approximated by

$$[S(IV)]_T = [S(IV)] + [RCH(OH)SO_3^-] \quad (19b)$$

and then

$$[S(IV)]_T = H_{SO_2} P_{SO_2} \left\{ 1 + \frac{K_{a1}}{[H^+]} \left(1 + K_1 H^* P_{RCHO} + \frac{K_{a2}}{[H^+]} \right) \right\} \quad (19c)$$

where H is the intrinsic Henry's law constant and $H^* = H/K_d + H$ (the effective Henry's law constant). H^* is not known for benzaldehyde but the reasonable assumption that the aqueous concentration of free benzaldehyde may typically be $0.2 \mu\text{M}$ has been made.³ Using this figure along with $P_{SO_2} = 20$ ppbv, $P_{HCHO} = 5$ ppbv, and $P_{MG} = 1$ ppbv, and application of eq 19c yields $[S(IV)]_T$ due to MG = 3 mM; $[S(IV)]_T$ due to HCHO = 50 μM ; and $[S(IV)]_T$ due to C₆H₅CHO = 0.5 μM . In the absence of any aldehydes (or other complexing agents) $[S(IV)]_T = 0.5 \mu\text{M}$. Thus, in spite of its lower concentration in naturally occurring water droplets, methylglyoxal could be a more important S(IV) reservoir than formaldehyde while benzaldehyde is unlikely to be an important reservoir. It is recognized that the assumptions made for these equilibrium calculations are simplistic but they nonetheless illustrate the remarkable potential for methylglyoxal to be an important S(IV) reservoir if it occurs at significant concentrations in the environment.

The data collected in Table VII show the effect of the electron-withdrawing power of R-, i.e., Taft's σ^* function, on the kinetic and thermodynamic properties of a series of aldehydes, R-CHO. In spite of the gaps in the table the data show that, in general, benzaldehyde is the only notable exception to the otherwise normal trend of CH_3CO- , H- > CH_3- , *i*-Pr-. This is probably due to resonance stabilization and perhaps also due to the steric effect associated with the bulky aromatic ring. Except for benzaldehyde, K_1 , the stability constant for reaction with HSO_3^- , decreases as σ^* decreases and R- is less able to stabilize the anionic α -hydroxysulfonate, R-CH(OH)SO₃⁻. Benzaldehyde also has an anomalously low rate of reaction with S(IV); k_1 and k_2 are lower than the corresponding values for formaldehyde.

These data indicate that, although acetaldehyde is common in polluted urban atmospheres,³⁶ it is probably not an important S(IV) reservoir because K_1 is relatively small and k_1 and k_2 are also likely to be small. (The concept of hyperconjugation can be used to explain the lower reactivity of acetaldehyde.) However, substitution on the methyl group with Cl to give chloral (and the mono- and disubstituted analogues), i.e., R = CCl₃-, has a marked effect on σ^* which would increase its affinity for S(IV). The reaction of chloral with S(IV) has not been studied in detail,³⁷ but since σ^* is so high it may show large rate constants and stability constants (if the steric effect of CCl₃- is not too large).

(39) (a) Greenzaid, P.; Luz, Z.; Samuel, D. *J. Am. Chem. Soc.* **1967**, *89*, 749-56. (b) Greenzaid, P.; Luz, Z.; Samuel, D. *Trans. Faraday Soc.* **1968**, *64*, 2780-6.

(40) Further indirect support comes from a consideration of the linear plots of $\log(1/K_d)$ vs. Taft's σ^* parameter which are also based on the assumption that the ketone carbonyl is unhydrated. If it were hydrated to a large extent then the linear correlation would break down since σ^* changes from 1.81 for $CH_3CO-CHO$ to 0.97 for $CH_3C(OH)_2-CHO$. This will be discussed in more detail in a subsequent paper.

It already has one of the key features for a good S(IV) reservoir, viz., a large hydration constant,²⁸ and it could thus be of significance in acidic fog and rain water if it occurred in the atmosphere. Halogenated aldehydes have not been found in the environment but halogenated hydrocarbons are common. The trends found in Table VII indicate that any aldehyde (or reactive ketone) which has a large σ^* and a small steric effect of R- and is found at significant concentrations could be a S(IV) reservoir. A good

example is hydroxyacetaldehyde (HOCH₂CHO) which has a much higher σ^* (0.62) than its parent, acetaldehyde (0.00), and which could also conceivably exist in the atmosphere.⁶ The hydroxyacetaldehyde-S(IV) system has not been studied.

Acknowledgment. We gratefully acknowledge the financial support of the Electric Power Institute (RP1630-47) and the Environmental Protection Agency (R811496-01-1).

Electronic Energy Transfer in Anisotropic Systems. 1. Octadecylrhodamine B in Vesicles

Lennart B.-Å. Johansson* and Alf Niemi

Department of Physical Chemistry, University of Umeå, S-901 87 Umeå, Sweden (Received: October 29, 1986; In Final Form: January 7, 1987)

Electronic energy transfer between octadecylrhodamine B (C₁₈RhB) solubilized in unilamellar vesicles of 1,2-dioleoyl-*sn*-glycero-3-phosphocholine (DOPC) has been studied. The quantum yield of fluorescence and the steady-state fluorescence anisotropy were measured at various temperatures and concentrations of C₁₈RhB. Rhodamine B chloride (RhB) has been used as a reference in the measurements of the quantum yield. For this purpose we found it necessary to determine the molar absorptivity and the fluorescence lifetime at different temperatures. The fluorescence decay of RhB in ethanol is monoexponential with a lifetime that continuously decreases from 3.6 ns at 265 K to 1.9 ns at 325 K. The radiative lifetime is 4.2 ns. From linear dichroism (LD) measurements we have determined the orientation of C₁₈RhB solubilized in macroscopically aligned lipid bilayers. No energy transfer could be detected when the mole fraction of C₁₈RhB in the vesicles was less than $\sim 10^{-4}$. Donor-donor and donor-acceptor (traps) transfers occur at concentrations higher than $\sim 10^{-4}$ and $\sim 10^{-3}$, respectively. The latter is most probably due to the formation of ground-state dimers of C₁₈RhB. Taken together, these experiments imply that the rate of energy transfer in anisotropic systems can be sensitive to and enhanced by the rotational motions of the interacting fluorophores.

Introduction

Radiationless transfer of electronic energy between atoms and molecules has been known for more than 50 years.¹ Forty years ago the pioneering work of Förster^{2,3} initialized the search for a model that quantitatively describes the macroscopically observed transfer among fluorescent molecules.

According to Förster's mechanism the rate of transfer depends on both the angular distribution and the spatial separation of the interacting molecules. Recently, a rigorous model was developed and tested for energy transfer in viscous solutions.^{4,5} In such systems the fluorophores undergo negligible rotational diffusion during the fluorescence lifetime and they are isotropically distributed which considerably simplifies the theoretical treatment. Few theoretical and experimental investigations deal with the problems associated with the transfer of electronic energy in *microscopically anisotropic* systems such as macromolecules or aggregates containing fluorophores, which are of fundamental interest not least for the understanding of photosynthetic units. The anisotropic motions and the orientational distribution of the fluorophores in such media will hence have an influence on the transfer rates. On the other hand, the spatial distribution function of the chromophores remains constant since the translational diffusion can be neglected on the time scale of fluorescence. Recently, a theoretical study of energy transfer in monolayer, bilayer, and multilayer systems has been presented.²² The rate of transfer was then assumed to be either very fast or very slow compared to the rotational motions of the interacting fluorophores. Fayer and co-workers have also experimentally studied energy transfer among octadecylrhodamine B solubilized in micelles.²³

In this work the energy transfer between octadecylrhodamine B (C₁₈RhB) solubilized in unilamellar vesicles of lipids has been investigated. The vesicles contain 1,2-dioleoyl-*sn*-glycero-3-phosphocholine (DOPC). The chromophoric part of C₁₈RhB is localized at the interface of the lipid bilayer so that interaction can occur both within this surface and across the bilayer. The transfer in this system is likely to be very similar to that in a planar lipid bilayer because a chromophore is very small compared to the size of a vesicle. The size distribution is unknown but should range in the order of tenths of nanometers which means that the transfer across a vesicle is negligible. There are advantages in using vesicles instead of micelles or liquid crystals as a model system in the study of energy transfer. The *local* concentration of the chromophore in the vesicles can be kept very high although the *total* concentration in the system is low. Furthermore, the energy transfer between vesicles can be omitted since the aggregate concentration is very low.

Materials and Methods

Rhodamine B chloride (pro analysi, Merck, W. Germany), octadecylrhodamine B chloride (Molecular Probes, Oregon) and 1,2-dioleoyl-*sn*-glycero-3-phosphocholine (DOPC, (>99%)), Synthesized at the Department of Physiological Chemistry, B.M.C., Uppsala, Sweden) were either freeze-dried for at least 2 days or heated in a drying pistol (Model TO-50, BüCHI, Switzerland) at 313 K for 3 h and further at room temperature for about 12 h. Water was quartz distilled and passed through Millipore filters (0.22 μ m). All solvents used were of spectroscopic grade.

Small unilamellar vesicles were prepared from DOPC as follows. A suspension of the lipid in water (≈ 3 mL) was sonicated (Branson sonicator B-30 equipped with a microtip) for periods of 5 min followed by 5 min of rest. The total time of sonication varied between 25 and 40 min depending on the amount of lipid. The samples were kept in a cooling bath at 263 K during the sonication. The sonicated vesicles were centrifuged at 97000g for 30 min.

(1) Perrin, J. *2me Conseil de Chim*; Solvay Gautier-Villars: Paris, 1925; p 322.

(2) Förster, Th. *Naturwissenschaften* **1946**, *33*, 166.

(3) Förster, Th. *Ann. Phys. Leipzig* **1948**, *2*, 55.

(4) Gochanour, C. R.; Andersen, H. C.; Fayer, M. D. *J. Chem. Phys.* **1979**, *70*, 4254.

(5) Gochanour, C. R.; Fayer, M. D. *J. Phys. Chem.* **1981**, *85*, 1989.